ACS Sustainable Chemistry & Engineering

Research Article

pubs.acs.org/journal/ascecg

Green Strategy Guided by Raman Spectroscopy for the Synthesis of Ammonium Carboxylated Nanocrystalline Cellulose and the Recovery of Byproducts

Edmond Lam, Alfred C. W. Leung, Yali Liu, Ehsan Majid, Sabahudin Hrapovic, Keith B. Male, and John H. T. Luong*

Building Montreal-Royalmount, National Research Council Canada, 6100 Royalmount Avenue, Montreal, Quebec, H4P 2R2 Canada

ABSTRACT: A one-pot green procedure for the treatment of cellulosic biomass with ammonium persulfate (APS) was developed for the synthesis of highly crystalline carboxylated nanocrystalline cellulose (NCC−COOH), an emerging nanomaterial with a plethora of diversified applications. Raman spectroscopy proved applicable for monitoring the fate of APS and its two byproducts during the production of NCC−COOH from microcrystalline cellulose (MCC). The two main byproducts were then identified and quantified as ammonium sulfate (AS) and H_2SO_4 with the latter accounted for 60% of the total sulfate ions in solution. On the basis of such findings, one-step neutralization of H_2SO_4 and NCC with NH_4OH immediately after reaction was implemented for the formation of additional AS, followed by its quantitative recovery by precipitation. This was a very effective and critical step in waste stream management and cost reduction for the large scale production of NCC. In addition, the process resulted in highly crystalline NCC with $COO^-NH_4^+$ groups, a nanomaterial with improved dispersion and thermal characteristics over NCC with COOH and COO^-Na^+ groups.

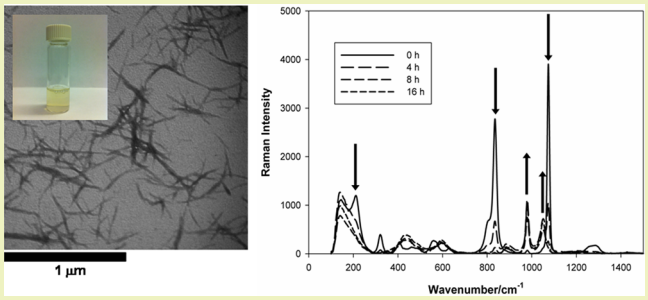

KEYWORDS: *Nanocrystalline cellulose, Raman spectroscopy, Persulfate, Sulfate, Sulfuric acid*

INTRODUCTION

Nanocrystalline cellulose (NCC), highly crystalline cellulose nanoparticles (1−100 nm in diameter and tens to hundreds of nanometers in length), can be processed from different sources of biomass using acid hydrolysis, enzymatic, or mechanical treatments to remove amorphous regions. As one of the strongest and stiffest natural materials available, NCC exhibits remarkable properties: high tensile strength (7500 MPa), high stiffness (Young's modulus of 100−140 GPa), high aspect ratio (70), large surface area (150−250 m^2/g), and other intriguing electrical and optical properties. NCC has received significant attention, and the synthesis, physical and optical properties, characterization, and application of NCC as a green material for biocomposites and relevant bioapplications have been widely reported.[1−6]

Recently, more homogeneous NCC (5 nm in diameter and 150 nm in length) has been prepared using ammonium persulfate (APS), a strong oxidant instead of conventional acid hydrolysis.[7,8] This versatile one-pot method can process a variety of cellulosic biomass without any pretreatments to remove noncellulosic plant contents such as lignin and hemicellulose. The use of APS results in the formation of carboxylated NCC compared to sulfonated NCC produced using mineral acids such as H_2SO_4. Although a mechanism was postulated involving the formation of $SO_4^{\bullet-}$, HSO_4^-, and hydrogen peroxide,[8] such byproducts were not identified and/or monitored during the course of NCC synthesis, due to time-consuming and tedious measurement with wet chemical analysis. In such studies, micrographs of NCC were simply characterized by transmission electron microscopy (TEM) and atomic force microscopy (AFM) to probe its dimension and homogeneity.[8]

This work demonstrates the applicability of Raman spectroscopy for probing the fate of APS and the formation of its inorganic byproducts during the course of an NCC-producing reaction.[9] These byproducts are then confirmed by thermogravimetric analysis (TGA), leading to a plausible mechanism for the synthesis of NCC by APS. In accordance to the Twelve Principles of Green Chemistry,[10] our procedure aims to further promote the use of renewal feedstocks for the production of nanocrystalline cellulose, while providing real-time analysis of persulfate degredation byproducts. A waste stream management strategy is then suggested for the recovery of such byproducts by precipitation to minimize waste and energy consumption, resulting in NCC with $COO^-NH_4^+$ groups, a highly dispersed and stable colloid compared to its parental carboxylated NCC.

Received: November 8, 2012
Revised: November 21, 2012
Published: December 17, 2012

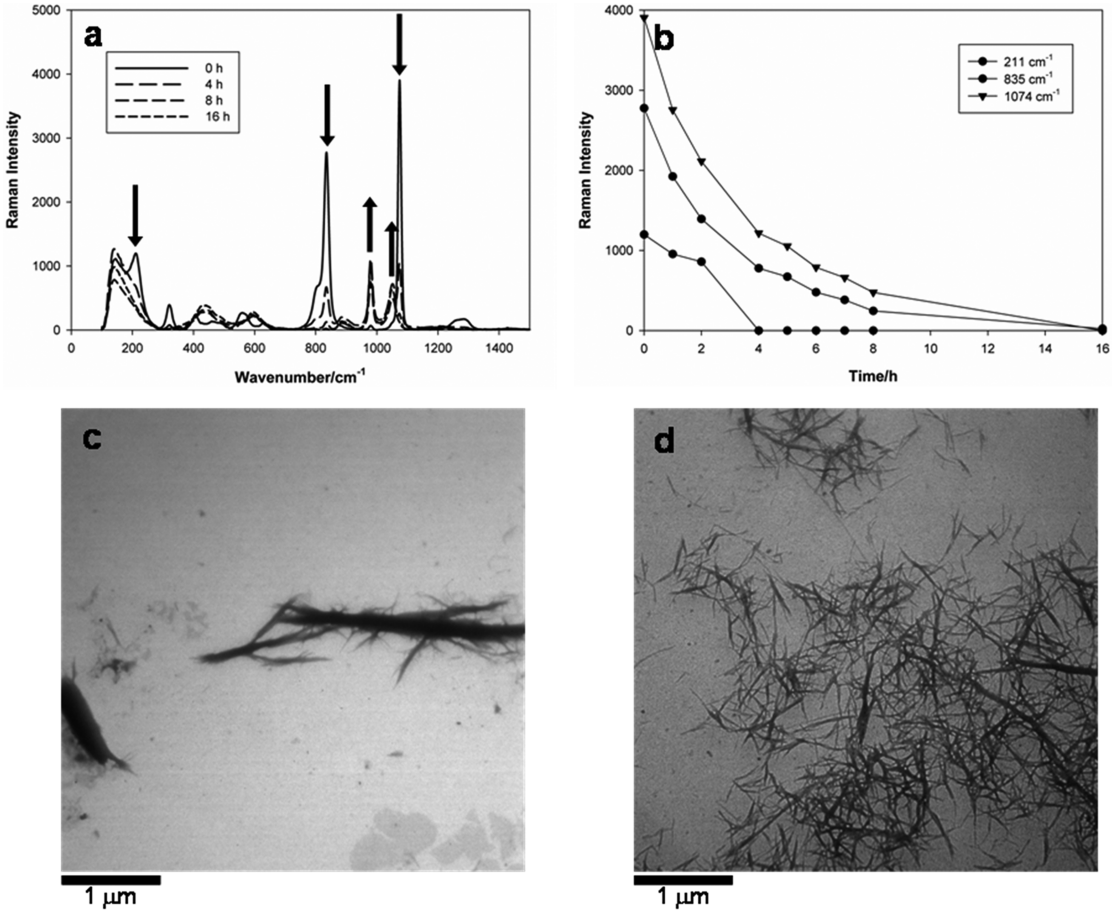

Figure 1. (a) Raman spectra and (b) Raman intensity count for the disappearance of APS in the reaction of 1% MCC in 1 M APS over 16 h at 60 °C. TEM images of cellulosic material at (c) 6 and (d) 16 h.

EXPERIMENTAL SECTION

Materials. Ammonium persulfate (APS), Avicel PH102 microcrystalline cellulose (FMC Corp.), ammonium sulfate (Aldrich), NH_4OH, H_2SO_4 (Fisher), and NaOH (EMD) were used as received.

Synthesis of NCC−COOH, NCC−COONa$^+$, and NCC−COONH$_4^+$. NCC−COOH and NCC−COONa$^+$ (NCC with COO^-Na^+ groups) were prepared and characterized by the literature method.[8] In brief, MCC (10 g) was hydrolyzed in 1 M APS (1 L) at 60 °C. Samples were taken every hour to determine the identity of byproducts by Raman spectroscopy. NCC−COONH$_4^+$ (NCC with $COO^-NH_4^+$ groups) was obtained by neutralizing the reaction mixture to pH 8 with liquid NH_4OH (125 mL). The white suspension was washed with H_2O, centrifuged three times at 10 000 rpm for 10 min, and freeze-dried to yield a white-colored product.

Characterization. Raman spectra were recorded using a Horiba/Jobin Yvon laser Raman analyzer LabRAM HR 800 (Horiba/Jobin Yvon, Longjumeau, France) equipped with a diode 784.8 nm laser (Sacher-TEC 510). The laser of the Raman spectrometric analyzer, integrated with a confocal microscope, was operated at approximately 125 mW using neutral density filters. The slit width was fixed at 1000 μm. A charge-coupled device (CCD) detector (open electrode) was operated at −75 °C, and the spectra were recorded with a resolution of 0.3 1/(cm pixel) of CCD due to the 800 mm focal length of the LabRAM HR. The instrument was wavelength-calibrated with a silicon wafer focused and collected as a static spectrum centered at 521 cm^{-1}. For assessing the reproducibility of this approach, five replicate spectra were obtained from each sample. The LabSpec software package (Horiba/Jobin Yvon) was used for the instrument control and data acquisition. ASCII data were exported from the LabSpec software into SigmaPlot.

Thermogravimetric analysis (TGA) was conducted with a Netzsch STA 449F1 (Netzsch Instruments, Burlington, MA, USA) at a heating rate of 10 °C/min from room temperature to 600 °C under helium purge gas. Low voltage transmission electron micrographs were obtained by a Delong LVEM (Soquelec, Montreal, QC, Canada) low-voltage TEM operating at 5 kV. A small amount of material (10 mg) was suspended in water (10 mL) and sonicated to disperse the material. A 4 mL drop of well-dispersed suspension was then dried on a Formvar-carbon coated grid and analyzed. Fourier transform infrared (FTIR) spectra were collected from samples in KBr from 4000 to 400 cm^{-1} for 64 scans at a resolution of 4 cm^{-1} (Bruker Tensor 27 FTIR spectrophotometer, Bruker Optics, Milton, ON, Canada). Dynamic light scattering and ζ-potential of the NCC materials (2 mg/mL) in water and were determined using a Zetasizer Nano-ZS (Malvern Instruments, Malvern, UK) in triplicate. Conductometric titration was conducted to determine the carboxylic acid content of NCC−COONH$_4^+$.[11] A Bruker D8-Advance X-ray diffractometer in Bragg−Brentano geometry with Cu Kα radiation (Cu Kβ was filtered out with a nickel screen) and a LynxEye detector was used for powder X-ray diffraction. Each sample was mixed with a little bit of water, spread evenly onto separate zero background silicon plates, and allowed to dry before scanning. The samples were scanned from 2θ = 5−70°, using a step size of 0.04°, and a total counting time of 216 s per step. The collected data were analyzed using WinPLOTR (http://www.llb.cea.fr/fullweb/winplotr/winplotr.htm), a graphics tool for powder diffraction to provide peak position (2θ), *fwhm* (full width half-maximum), peak deconvolution, and integration intensity for calculation of the crystallinity index (CRI). The average crystal size is estimated as $K\lambda/(\text{fwhm} \times \cos\theta)$ with the form factor or Scherrer constant (K) taken as 1 and λ = 1.54184 Å.

dx.doi.org/10.1021/sc3001367 | ACS Sustainable Chem. Eng. 2013, 1, 278−283

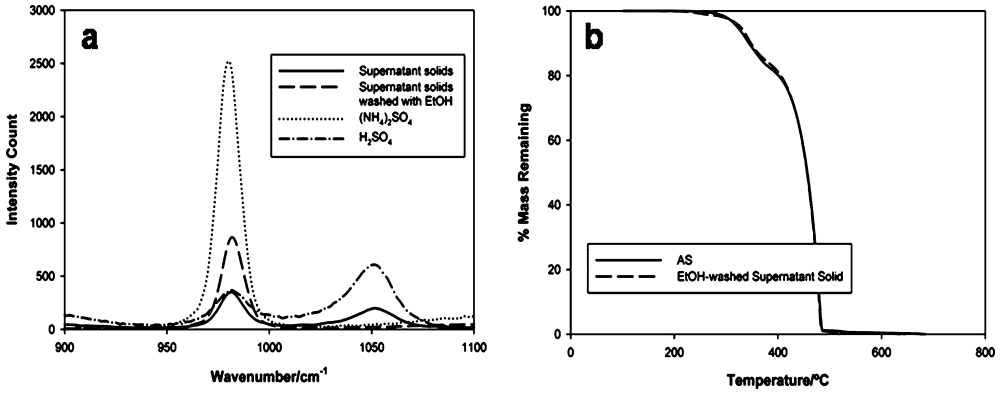

Figure 2. (a) Raman spectra identifying the sulfur-containing species from solids obtained by evaporating the 16 h supernatant sample to dryness. (b) TGA plots confirming that the EtOH-washed supernatant solid is AS.

RESULTS AND DISCUSSION

Decomposition of APS. APS has been known to exhibit three major Raman peaks: 211 cm^{-1} (δ_m: deformational vibration of the S−O−O−S bridge), 835 cm^{-1} (ν_m: symmetric stretching vibration of the S−O−O−S bridge), and 1074 cm^{-1} (ν_s: symmetric stretching vibration of the S−O bond of the SO_3^- group of the persulfate anion).[12] When the APS solution is subject to heat treatment,[12] the cleavage of the peroxide bond of APS, the weakest bond, is expected to generate two SO_4^- radical ions ($S_2O_8^{2-}$ + heat → $2SO_4^{\bullet-}$). Under the acidic conditions, hydrogen peroxide will also be formed ($S_2O_8^{2-}$ + $2H_2O$ → $2HSO_4^-$ + H_2O_2).[8] As shown in Figure 1a, when 1% MCC was heated to 60 °C in 1 M APS, the Raman peaks of APS at 211 and 1074 cm^{-1} began to diminish as the O−O bond of the persulfate cleaved to give two $SO_4^{\bullet-}$ radical anions.[12] Of interest was the disappearance of the characteristic peak at 211 cm^{-1} after 4 h into the experiment whereas the peaks at 835 and 1074 cm^{-1} only disappeared after 16 h, corresponding to the total time required for the synthesis of homogeneous NCC with good yields (Figure 1b). Such results unraveled that APS was rapidly decomposed to form $SO_4^{\bullet-}$ and HSO_4^- free radicals which in turn cohydrolyzed the 1,4-β bond of the cellulose chain in the amorphous region, resulting in the formation of NCC.[8] Together with hydrogen peroxide, these two free radicals were capable of oxidizing −CH_2OH in the C_6 position to form COOH groups on the NCC surface.[8] The TEM micrograph in Figure 1c confirmed that only few NCC were synthesized after 6 h into the experiment whereas most of the MCC starting material remained intact. After 16 h, most of the MCC was hydrolyzed to NCC with approximately 5 nm in diameter and 150 nm in length (Figure 1d).

Identification of Inorganic Byproducts. The reaction liquid containing MCC and APS also displayed two emerging peaks with increasing intensities at 980 and 1051 cm^{-1} as the reaction progressed to completion in 16 h (Figure 1a). As a well-known model of "free" sulfate systems, an aqueous ammonium sulfate (AS) solution exhibits a $\nu_1(SO_4^{2-})$ band with only a small red shift from 981 to 977 cm^{-1} when the water−solid ratio decreases from 15.8 to 1.7.[13] Sulfuric acid also exhibits a $\nu_1(SO_4^{2-})$ band at 982 cm^{-1}, with additional Raman bands at 890 cm^{-1} (ν(SOH): asymmetric stretching vibration of HSO_4^-) and 1040 cm^{-1} (ν_1: symmetric stretching vibration of HSO_4^- ions). The band intensity and frequency of these three peaks are also dependent upon the acid concentration.[14] Above 80 wt %, sulfuric acid has been known to exhibit only two prominent Raman peaks at ∼910 (ν(SOH)) and ∼1050 cm^{-1} (ν_s).[14]

For the confirmation of AS and sulfuric acid as two major byproducts, the reaction mixture obtained after 16 h was centrifuged to separate NCC from the reaction liquid. The resulting supernatant was evaporated to dryness, leaving a white, semimolten solid with two Raman peaks at 980 and 1051 cm^{-1} (Figure 2a). The peak at 980 cm^{-1} could be assigned as the $\nu_1(SO_4^{2-})$ band of AS. Although sulfuric acid displays a similar Raman band at this frequency, the intensity of this peak decreases with increasing H_2SO_4 concentration. This peak almost vanishes when the acid concentration is above 80 wt %, where low water content prevents H_2SO_4 from ionizing into H_3O^+ and HSO_4^- or $2H_3O^+$ and SO_4^{2-}.[14] Therefore, the peak at 980 cm^{-1} was unlikely attributed to the presence of sulfuric acid, based on the experimental conditions conducted in this study. Nevertheless, the emerging second peak (ν_s) observed at 1051 cm^{-1} attested the formation of sulfuric acid as a second major byproduct during the synthesis of NCC using APS.

The experiment was then conducted to separate AS from sulfuric acid in the supernatant, a key step to byproduct recovery to improving economic viability for large-scale NCC−COOH production. Owing to the insolubility of AS in alcohols, EtOH was added to the supernatant to precipitate out AS. It should be noted that EtOH was selected over other organic solvents including acetone and acetonitrile to its availability, lower toxicity, and greatest efficiency. Further drying of the EtOH-washed solid resulted in a mass loss of 67% attributed to the removal of H_2SO_4. The Raman spectrum and thermogravimetric analysis (TGA) (Figure 2b) confirmed the identity of the EtOH-precipiated solid as AS. TGA of AS and the EtOH-washed solid both showed two decomposition steps centered on 297 and 392 °C.[15] In a control experiment, ∼3 equiv of EtOH was required to precipitate out 95% of AS in a 1 M aqueous solution of AS.

A pH of less than 2 for the supernatant, together with the aforementioned information, strongly suggested that a large proportion of sulfate ions in the solution exist as H_2SO_4. Therefore, the supernatant obtained at 16 h containing both AS and sulfuric acid was neutralized with NH_4OH to pH 8 to effect the formation of additional AS from H_2SO_4. The resulting liquid was precipitated with 3 equiv of EtOH, followed by drying and subjected to Raman and TGA analyses. Again, this powder exhibited the Raman signature of AS with 94% of the AS recovery, based on the amount of APS used in the experiment (Figure 3).

dx.doi.org/10.1021/sc3001367 | ACS Sustainable Chem. Eng. 2013, 1, 278−283

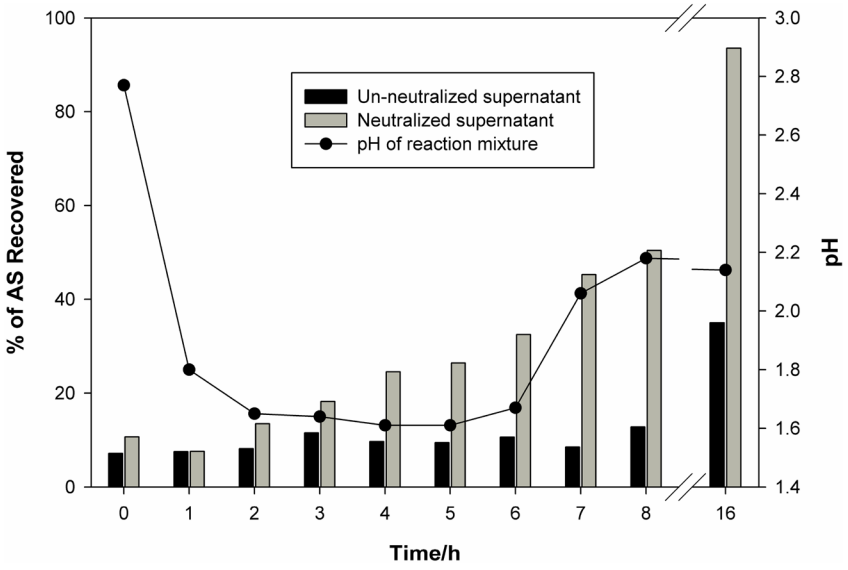

Figure 3. AS recovery from un-neutralized and neutralized supernatant (using NH_4OH) from the reaction of 1% MCC with 1 M APS.

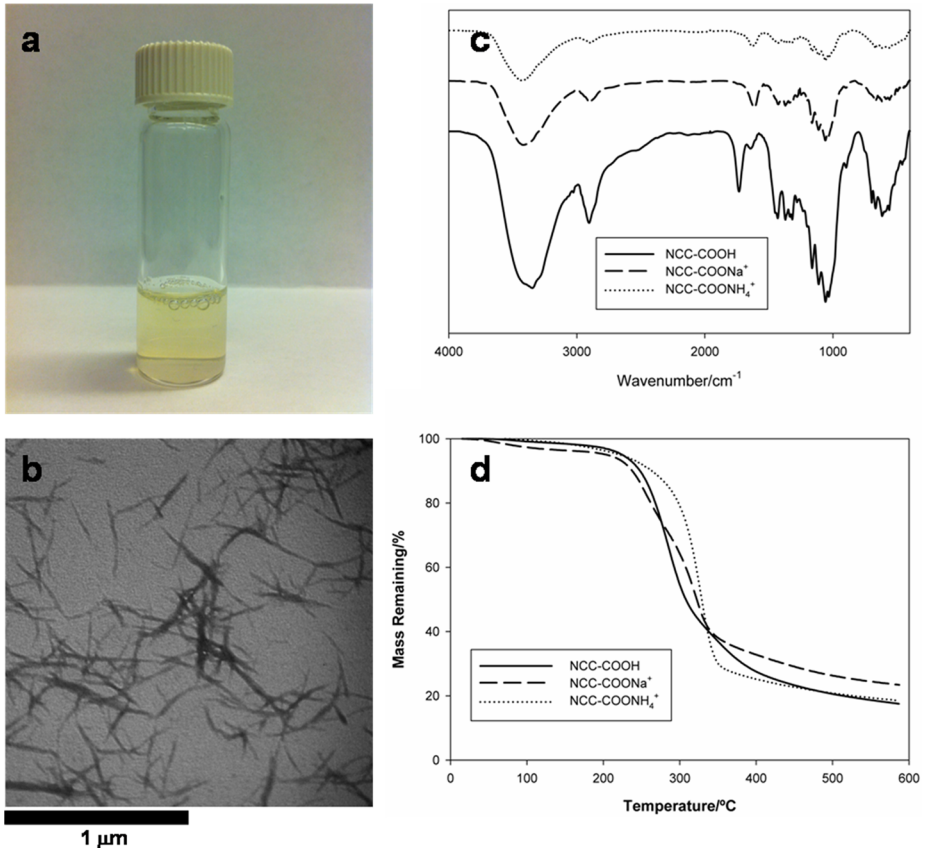

Figure 4. (a) 5 wt % solution of NCC−$COONH_4^+$ in water. (b) TEM image of NCC−$COONH_4^+$. (c) FTIR spectra and (d) TGA plots of NCC−COOH, NCC−$COONa^+$, and NCC−$COONH_4^+$.

Alternatively, a series of experiments was also conducted to regenerate APS from AS by electrochemical oxidation[16−18] using a boron doped diamond electrode as the anode and a Pb electrode as the cathode. A two-compartment electrochemical cell was divided by Nafion membrane in order to separate anodic from cathodic reaction and preserve any regenerated APS. It was found that the regeneration must be performed at a lower temperature of 15 °C to prevent the degradation of APS in comparison to 60 °C for the synthesis of NCC. The current density needed for this reaction was 15−20 mA/cm^2 with an applied potential of 20−25 V. However, under these conditions, this electrochemical method not amenable for industrial applicability due to considerable heat formation and insignificant quantities of APS regenerated in situ as determined by Raman spectroscopy.

dx.doi.org/10.1021/sc3001367 | ACS Sustainable Chem. Eng. 2013, 1, 278−283

Simultaneous Recovery of Byproducts with Formation of NCC−$COONH_4^+$. The production of NCC from APS produces NCC−COOH in which the product was isolated by washing with water to remove residuals salts and freeze-dried to give a white powder. To improve their redispersion into water, NCC−COOH has been neutralized with NaOH to yield NCC−$COONa^+$.[8] In this work, NH_4OH was added to a completed NCC−COOH producing reaction (1% MCC in 1 M APS, heated to 60 °C for 16 h), to bring the pH of the solution to 8. NCC−$COONH_4^+$ (NCC with $COO^-NH_4^+$ groups) was washed and centrifuged with water and then freeze-dried to give a white powder with an isolated yield of 29%. NCC−$COONH_4^+$ is easily dispersed into water as a 5 wt % solution with 500 J of sonication (Figure 4a). NCC−$COONH_4^+$ was characterized by TEM, FTIR, and TGA (Figures 4b−d). Similar to previously prepared NCC−COOH and NCC−$COONa^+$,[8] NCC−$COONH_4^+$ has nanoscale dimensions. FTIR spectra of the different NCC materials show distinct ν(C═O) stretching peaks from 1733 (COOH) to 1613 (COO^-Na^+) and 1628 cm^{-1} ($COO^-NH_4^+$), respectively.

Thermal stability of NCC is important for thermoplastics applications since the processing temperature is often above 200 °C. TGA plots of the three NCC materials show different decomposition patterns. From 40 to ∼120 °C, the weight loss was due to water evaporation in the samples. A plateau then appeared until 260 °C because cellulose usually undergoes degradation at temperatures ranging from 250 to 400 °C.[19] Complete decomposition of NCC to volatile products including CO_2 was observed at >400 °C that could be attributed to the depolymerization and decomposition of the cellulose chain. It should be noted that the T_{d5} (the degradation temperature of 5% weight loss) for NCC−$COONH_4^+$ of 221 °C was comparable to that of NCC−COOH at 224 °C. Both nanomaterials were appreciably higher than the T_{d5} of NCC−$COONa^+$ at 204 °C.

Figure 5 shows the diffractograms of the NCC materials characterized by X-ray diffraction (XRD). All three materials exhibit two intense peaks at 2θ = 22.7° for the (002) peak and 15.1° for the (101) peak. A slight shoulder centered at 2θ = 16.5° represents the lower peak (10−1). The diffraction patterns, including the d_{hkl}-spacing and average crystallite size as determined by the Debye−Scherrer formula are characteristic for cellulose I structure. The average crystallite size for the 3 NCC samples was estimated to be 2.95 (SD ± 1.35), 2.89 (SD ± 1.34), and 2.59 nm (SD ± 1.13 nm) for NCC−COOH, NCC−$COONa^+$, and NCC−$COONH_4^+$.The crystallinity index (CRI) of the NCC materials was estimated using an integral method based on the ratio of the crystalline area to total scattered intensity. The CRIs of NCC−COOH, NCC−$COONa^+$, and NCC−$COONH_4^+$ were 77.7%, 78.1%, and 74.5%, respectively, An alternative method to determining the CRI is to calculate the height ratio between the intensity value ($I_{002} - I_{AM}$) and total intensity (I_{002}) after subtraction of the background signal measured without cellulose.[20] I_{002} is the intensity obtained from the (002) peak while I_{AM} is the minimum intensity found between the (101) and (002) peaks. From this method, the CRIs of NCC−COOH, NCC−$COONa^+$, and NCC−$COONH_4^+$ were 81.7%, 80.8%, and 74.8%, respectively. The CRI values obtained from both methods imply that the crystallinity of the NCC−COOH remained unchanged in the presence of different cations, i.e., when it was subject to neutralization by NaOH or NH_4OH.

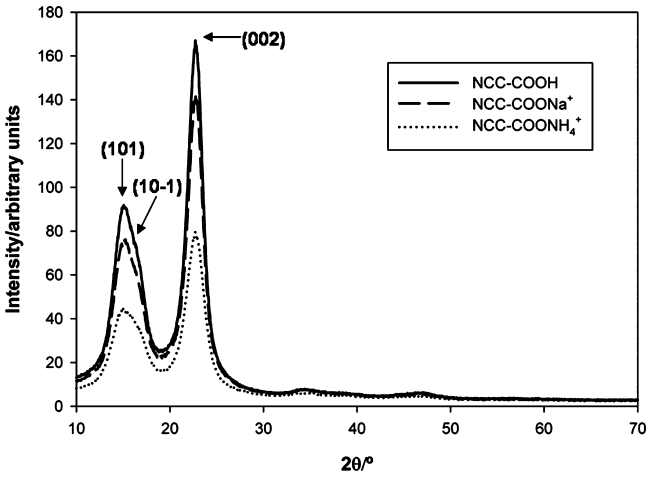

Figure 5. XRD diffractograms of NCC−COOH, NCC−$COONa^+$, and NCC−$COONH_4^+$. Note that the intensity of the diffractograms is dependent on sample preparation prior to XRD analysis. CRI values were obtained from the ratio of peak area or intensity values.

NCC−$COONH_4^+$ (2 mg/mL solution in water) gave the ζ-potential of −43.3 ± 2.3 mV in comparison to −20.4 ± 2.6 mV for NCC−$COONa^+$ (2 mg/mL solution in water). Such results attested more hydrophilicity of NCC−$COONH_4^+$ over NCC−$COONa^+$ since high ζ-potential (negative or positive above 40 mV) will confer stability of a colloid dispersion.[21] This was an important finding as highly dispersed NCC is a critical property for its uniform incorporation as a reinforcing agent in biocomposites.

For the determination of the degree of oxidation (DO), NCC−$COONH_4^+$ was subject to 0.1 M HCl for complete protonation of the COOH groups, i.e., NCC−$COONH_4^+$ → NCC−COOH. After dialysis and freeze-drying, the resulting NCC−COOH was titrated with NaOH and the DO value was calculated using the following equation:

$$\mathrm{DO} = \frac{162(V_2 - V_1)C}{w - 14(V_2 - V_1)C}$$

where C is the NaOH concentration (M), w is the weight of freeze-dried NCC sample (g), and V_1 and V_2 are the volumes of NaOH (L). The molecular weight of an anhydroglucose unit (with CH_2OH group) is 162. The molecular weight difference between an anhydroglucose unit and its COOH derivative is 14.

As shown in Figure 6, the neutralization of the carboxylic acid groups in a 50 mg sample (w) of fully protonated NCC−COOH required 2.93 mL of NaOH (0.01 M), corresponding to the DO value of 0.096. The reproducibility of this procedure this experiment was excellent with a DO of 0.094 obtained in a second experiment. FTIR spectra can also be conveniently used for the estimation of the DO of the fully protonated NCC−$COONH_4^+$, corresponding to the ratio of the intensity of the absorbance bands at 1726 cm^{-1} (ν(C═O) in the acid form) and 1033 cm^{-1} (cellulose backbone).[22] From Figure 6 (inset), the *DO* value of 0.096 obtained by FTIR was in agreement with conductometric titration.

From a theoretical viewpoint for the maximum degree of oxidation of NCC, one can consider a fully oxidized individual nanocrystal with square sectional dimensions of 5 nm × 5 nm. If n is the number of cellulose chains per side of the crystal,

dx.doi.org/10.1021/sc3001367 | ACS Sustainable Chem. Eng. 2013, 1, 278−283

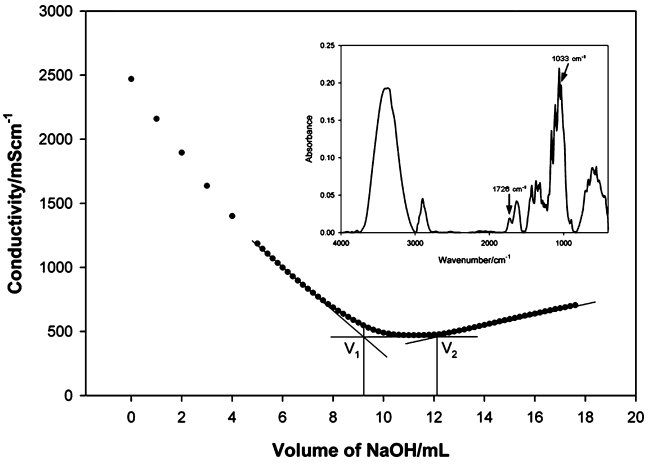

Figure 6. Conductometric titration curve of fully protonated NCC−COOH where the DO = 0.096. (inset) FTIR absorbance spectrum of fully protonated NCC−COOH.

then n^2 is the number of chains in the crystal and the number of surface chains is $4(n-1)$. Thus, the ratio (r) of surface chains to the total number of cellulose chains in the crystal can be calculated as $r = 4(n-1)/n^2$. If the maximum DO is relative only to the surface oxidation and only every second surface hydroxymethyl group can be oxidized, the DO value should be $r/2$. Taking an average value of 0.57 nm between cellulose chains within the (110) and (1−10) faces of the crystal,[22] the maximum DO of a 5 nm × 5 nm square crystal is ∼0.20 (with n = 9). Considering the DO value obtained by FTIR or conductometric titration, one might conclude that about 50% of the surface hydroxymethyl group was oxidized to COOH during the course of NCC synthesis.

CONCLUSIONS

The applicability of Raman spectroscopy has been proven for monitoring and identification of the two main byproducts formed during the production of carboxylated NCC (NCC−COOH) from MCC using APS. Nearly 60% of the sulfate ions in solution exist as H_2SO_4 with the remainder existing as ammonium sulfate. Near quantitative recovery of AS was achieved by neutralization of the reaction with NH_4OH followed by precipitation with EtOH. Consequently, NCC−$COONH_4^+$ with nanoscale dimensions was synthesized with improved dispersion and thermal stability in water which could be functionalized for diversified applications in aqueous or solvent systems. Raman spectroscopy can be equipped with a miniature probe for process monitoring and this could serve as a useful tool to follow the kinetics of the APS oxidation and decomposition.

AUTHOR INFORMATION

Corresponding Author

*E-mail address: john.luong@cnrc-nrc.ga.ca. Telephone: +1 514 496 6175. Fax: +1 514 496 6265.

Notes

The authors declare no competing financial interest.

REFERENCES

(1) Habibi, Y.; Lucia, L. A.; Rojas, O. J. Cellulose Nanocrystals: Chemistry, Self-Assembly, and Applications. *Chem. Rev.* **2010**, *110* (6), 3479−3500.

(2) Moon, R. J.; Martini, A.; Nairn, J.; Simonsen, J.; Youngblood, J. Cellulose nanomaterials review: structure, properties and nanocomposites. *Chem. Soc. Rev.* **2011**, *40* (7), 3941−3944.

(3) Ramires, E. C.; Dufresne., A. A review of cellulose nanocrystals and nanocomposites. *TAPPI* **2011**, *10*, 9−16.

(4) Klemm, D.; Kramer, F.; Moritz, S.; Lindström, T.; Ankerfors, M.; Gray, D.; Dorris, A. Nanocelluloses: A new family of nature-based materials. *Angew. Chem., Int. Ed.* **2011**, *50* (24), 5438−5466.

(5) Holt, B. L.; Stoyanov, S. D.; Pelan, E.; Paunov, V. N. Novel anisotropic materials from functionalised colloidal cellulose and cellulose derivatives. *J. Mater. Chem.* **2010**, *20* (45), 10058−10070.

(6) Lam, E.; Male, K. B.; Chong, J. H.; Leung, A. C. W.; Luong, J. H. T. Applications of Functionalized and Nanoparticle Modified Nanocrystalline Cellulose. *Trends Biotechnol.* **2012**, *30* (5), 283−290.

(7) Leung, C. W.; Luong, J. H. T.; Hrapovic, S.; Lam, E.; Liu, Y.; Male, K. B.; Mahmoud, K.; Rho, D. *Cellulose nanocrystal from renewable biomass*. National Research Council of Canada, Canada; CA 2010/000372; 2011.

(8) Leung, A. C. W.; Hrapovic, S.; Lam, E.; Liu, Y.; Male, K. B.; Mahmoud, K. A.; Luong, J. H. T. Characteristics and properties of carboxylated cellulose nanocrystals prepared from a novel one-step procedure. *Small* **2011**, *7* (3), 302−305.

(9) Degen, I. A.; Newman, G. A. Raman spectra of inorganic ions. *Spectrochim. Acta* **1993**, *49A* (5−6), 859−887.

(10) Anastas, P. T.; Warner, J. C. *Green Chemistry: Theory and Practice*; Oxford University Press: New York, 1998.

(11) Saito, T.; Nishiyama, Y.; Putaux, J.-L.; Vignon, M.; Isogai, A. Homogeneous suspensions of individualized microfibrils from TEMPO-catalyzed oxidation of native cellulose. *Biomacromolecules* **2006**, *7* (6), 1687−1691.

(12) Vorsina, I. A.; Mikhailov, Y. I. Kinetics of thermal decomposition of ammonium sulfate. *Russ. Chem. Bull.* **1996**, *45* (3), 539−542.

(13) Zhang, Y. -H.; Chan, C. K. Understanding the hygroscopic properties of supersaturated droplets of metal and ammonium sulfate solutions using Raman spectroscopy. *J. Phys. Chem. A* **2002**, *106* (2), 285−292.

(14) Tomikawa, K.; Kano, H. Raman study of sulfuric acid at low temperatures. *J. Phys. Chem. A* **1998**, *102* (30), 6082−6088.

(15) Kiyoura, R.; Urano, K. Mechanism, Kinetics, and Equilibrium of Thermal Decomposition of Ammonium Sulfate. *Ind. Eng. Chem. Process Des. Develop.* **1970**, *9* (4), 489−494.

(16) Serrano, K.; Michaud, P. A.; Comninellis, C.; Savall, A. Electrochemical preparation of peroxodisulfuric acid using boron doped diamond thin film electrodes. *Electrochim. Acta* **2002**, *48* (4), 431−436.

(17) Radimer, K. J.; McCarthy, M. J. *Electrolytic production of sodium persulfate*. FMC Corporation, USA; US Patent 4,144,144, March 13, 1979.

(18) Dong, D. F.; Mumby, T. A.; Jackson, J. R.; Rogers, D. J. *Co-generation of ammonium persulfate anodically and alkaline hydrogen peroxide cathodically with cathode products ratio control*. Huron Tech Canada Inc., Canada; US Patent 5,643,437, July 1, 1997.

(19) Higgins, H. G. The degradation of cellulose in air at 250°C as shown by infrared spectroscopic examination. *J. Polym. Sci.* **1958**, *28* (118), 645−648.

(20) Segal, L.; Creely, J. J.; Martin, A. E.; Conrad, C. M. An empirical method for estimating the degree of crystallinity of native cellulose using the X-ray diffractometer. *Tex. Res. J.* **1962**, *29* (10), 786−794.

(21) Hunter, R. J. *Foundations of Colloid Science*; Oxford University Press, Oxford, 1989.

(22) Habibi, Y.; Chanzy, H.; Vignon, M. TEMPO-mediated surface oxidation of cellulose whiskers. *Cellulose* **2006**, *13* (6), 679−687.